Stem Cell Reports
Article

ISSCR

OPEN ACCESS

Efficient generation of dopaminergic induced neuronal cells with midbrain characteristics

Yi Han Ng,[1,2,3,4] Soham Chanda,[1,3,5] Justyna A. Janas,[1] Nan Yang,[1,6] Yuko Kokubu,[1] Thomas C. Südhof,[3] and Marius Wernig[1,*]

[1]Institute for Stem Cell Biology and Regenerative Medicine and Department of Pathology, Stanford University School of Medicine, Stanford, CA 94305, USA
[2]Department of Microbiology and Immunology, Stanford University School of Medicine, Stanford, CA 94305, USA
[3]Department of Molecular and Cellular Physiology and Howard Hughes Medical Institute, Stanford, CA 94305, USA
[4]Present address: Laboratory of Metabolic Medicine, Singapore Bioimaging Consortium, Agency for Science, Technology and Research, Singapore, Singapore
[5]Present address: Department of Biochemistry and Molecular Biology, Colorado State University, Fort Collins, CO 80523, USA
[6]Present address: Department of Neuroscience, Friedman Brian Institute, Black Family Stem Cell Institute, Icahn School of Medicine at Mount Sinai, NY 10029, USA
*Correspondence: wernig@stanford.edu
https://doi.org/10.1016/j.stemcr.2021.05.017

SUMMARY

The differentiation of pluripotent stem cells can be accomplished by sequential activation of signaling pathways or through transcription factor programming. Multistep differentiation imitates embryonic development to obtain authentic cell types, but it suffers from asynchronous differentiation with variable efficiency. Transcription factor programming induces synchronous and efficient differentiation with higher reproducibility but may not always yield authentic cell types. We systematically explored the generation of dopaminergic induced neuronal cells from mouse and human pluripotent stem cells. We found that the proneural factor *Ascl1* in combination with mesencephalic factors *Lmx1a* and *Nurr1* induce peripheral dopaminergic neurons. Co-delivery of additional midbrain transcription factors *En1*, *FoxA2*, and *Pitx3* resulted in facile and robust generation of functional dopaminergic neurons of midbrain character. Our results suggest that more complex combinations of transcription factors may be needed for proper regional specification of induced neuronal cells generated by direct lineage induction.

INTRODUCTION

Pluripotent stem cells (PSCs) have been heralded to hold great potential for applications in regenerative medicine. Embryonic stem cells (ESCs) and induced PSCs (iPSCs) can differentiate into any type of tissues and cells, making them a promising source for regenerative medicine (Blanpain et al., 2012; Hanna et al., 2010; Okita and Yamanaka, 2011). While very versatile, pluripotency also creates a major challenge, as only well-differentiated populations of typically only one cell type in high purity are suitable for transplantation-based approaches. Contamination of undesired cell types may cause unexpected complications such as tumor formation. Two principal approaches have been used to differentiate pluripotent cells: (1) use of extracellular differentiation cues mimicking signaling pathway activation during embryonic development and (2) experimental expression of lineage-determining transcription factors (TFs) (Chambers et al., 2009; Kriks et al., 2011; Maroof et al., 2013; Merkle et al., 2015; Yamamizu et al., 2013; Zhang et al., 2013). The latter approach has also been applied to non-pluripotent cell populations (Berninger et al., 2007; Marro et al., 2011; Qian et al., 2012; Vierbuchen et al., 2010).

The generation of authentic midbrain dopamine neurons represents a major goal in regenerative medicine research because the transplantation of such cells can improve motor deficits in Parkinson's disease whereas improperly specified dopamine neurons are believed to have limited therapeutic value (Lindvall and Bjorklund, 2011). Intensive research over the last decades has resulted in remarkable advances in optimizing the "conventional" extracellular stimulation-based approach, almost reaching clinical grade levels (Kriks et al., 2011; Xi et al., 2012). The "induced neuronal (iN) cell" approach, based on expression of TFs, has only recently been described and applied to PSCs. With respect to generating glutamatergic neurons, we observed that the iN cell system is very efficient and reproducible (Pang et al., 2011; Vierbuchen et al., 2010; Zhang et al., 2013). Also, a number of groups reported the generation of tyrosine hydroxylase (TH)-positive (TH^+) dopamine neurons from both fibroblasts and ESCs, but their proper regionalization has not yet been investigated (Caiazzo et al., 2011; Kim et al., 2011; Pfisterer et al., 2011; Theka et al., 2013). Here we observed that many TF combinations fail to induce the proper central, midbrain identity in TH^+ neurons. However, the lack of appropriate regional specification appears to be not a problem of the iN cell approach in principle, since further addition of specific TFs resulted in induced dopamine neurons with central nervous system (CNS) characteristics.

RESULTS

The proneural bHLH transcription factor *Ascl1* is sufficient to induce TH$^+$ iN cells from mouse and human ESCs

We previously reported that the proneural basic helix-loop-helix (bHLH) TF *Ngn2* could efficiently and rapidly induce neuronal cells from human ESCs and iPSCs (Zhang et al., 2013). These iN cells derived from pluripotent cells were a homogeneous population of excitatory neurons and showed functional maturation levels far exceeding iN cells generated from human fibroblasts (Pang et al., 2011; Pfisterer et al., 2011; Yoo et al., 2011). As *Ngn2* is expressed in progenitor domains giving rise to excitatory neurons, we speculated that addition or replacement with other lineage-determination factors could induce other cell fates. We tested this hypothesis by attempting to generate cells resembling midbrain-type dopamine neurons. Since those cells are considered to be excitatory (Chuhma et al., 2004; Sulzer et al., 1998), we first assessed dopamine neuron marker expression in *Ngn2* embryonic stem cell (ES)-iN cells. We generated cells as previously described (Figures 1B and S1A) (Zhang et al., 2013) and immunostained the cultures for TH$^+$ cells. We observed that only exceedingly rare *Ngn2* iN cells were immunoreactive (Figures 1C and 1E).

Recently we had observed that *Ascl1*, another proneural bHLH TF with a different expression pattern, can generate iN cells from mouse and human ESCs as well (Chanda et al., 2014). While the reprogramming kinetics was different, the ultimately resulting *Ascl1* iN cells were also excitatory and similar to the *Ngn2* iN cells. Nevertheless, we wondered whether these cells might differ in dopamine marker expression. In contrast to *Ngn2* ES-iN, a much higher fraction of *Ascl1*-mediated ES-iN cells was TH$^+$ from both mouse and human ESCs (Figures 1A–1C, 1E, and S1). As mouse ESCs are difficult to infect, we used an *Ascl1*-inducible mouse ESC line to generate iN cells for our characterization (Figure S1) (Chanda et al., 2014; Wapinski et al., 2013).

We observed that these *Ascl1*-mediated TH$^+$ iN cells still had immature morphologies (Figure 1C). We therefore added *Myt1l*, another previously discovered reprogramming TF with a pan-neuronal expression pattern and, thus, likely to promote proneuronal differentiation and maturation rather than influencing subtype specification (Vierbuchen et al., 2010). The addition of *Myt1l* did not change the overall ratio of TH$^+$ cells after 3 weeks (Figures 1C and 1E). A closer assessment of *Myt1l* maturation effects revealed that there was indeed an increased complexity of the *Myt1l*-transduced cells on day 5 (Figure S1C), but after 3 weeks we could not detect any morphological differences based on quantification of the mean branches per cell and mean processes per cell (Figure S1D), similar to our previous results with fibroblasts and in the context of generation of GABAergic neurons by *Ascl1* and *Dlx2* (Chanda et al., 2014; Yang et al., 2017).

Addition of the dopamine transcription factors *Nurr1* and *Lmx1a* does not increase the ratio of TH$^+$ cells

It was previously suggested that the combined expression of *Ascl1*, *Nurr1*, and *Lmx1a* (ANL) effectively induces TH$^+$ cells from fibroblasts and ESCs (Caiazzo et al., 2011; Theka et al., 2013). We therefore compared this combination with *Ascl1*-only-infected and *Ascl1*, *Myt1l* (AM)-infected ES-iN cells. Unexpectedly, we did not observe a significant difference in the proportion of TH$^+$ cells among all MAP2$^+$ iN cells (Figures 1D and 1E). Expression of the TFs in the cells was verified by protein immunoreactivity or immunoblotting (Figures S1E–S1G). The addition of *Nurr1* and *Lmx1a* to *Ascl1*, if anything, slightly decreased the fraction of TH$^+$ cells (Figure 1E). This observation suggests that at least in ESCs, *Ascl1* is sufficient to induce neurons with a small proportion of TH$^+$ cells, and the addition of the midbrain-specific TFs *Nurr1* and *Lmx1a* does not further support the induction of TH$^+$ cells by *Ascl1*.

TH$^+$ ES-iN cells derived by *Ascl1* with or without *Nurr1* and *Lmx1a* express peripheral markers and lack midbrain markers

The enzyme TH is a critical but not absolutely specific marker of midbrain dopamine neurons. Peripheral neurons, such as the secondary neurons of the peripheral sympathetic nervous system or neurons within the enteric system, require TH for catecholamine biosynthesis and stain positive for this marker (Eisenhofer et al., 2004). Of note, while *Ascl1* plays important roles in the CNS, it is also an essential factor for peripheral neurons such as the autonomic nervous system (Guillemot et al., 1993). We therefore decided to further characterize the TH$^+$MAP2$^+$ double-positive cells obtained from ESCs and analyzed their co-expression of additional markers indicating their regional specification. We found that a substantial proportion of the TH$^+$ (46%) mouse ES-iN cells derived with *Ascl1* co-expressed the peripheral marker peripherin (PRPH) (Figure 2A). We confirmed PRPH specificity by immunostaining sagittal sections of the adult mouse brain (Figure S2). While we did observe some immunoreactive fibers in the brainstem (presumably derived from cranial nerve cells), the TH$^+$ cells in the CNS were clearly devoid of PRPH (Figures S2A–S2D). Moreover, primary cortical cultures derived from neonatal mouse brains were also devoid of PRPH$^+$ cells. Thus, we are confident that the detection of PRPH in the ES-iN cells is indicative of a peripheral identity.

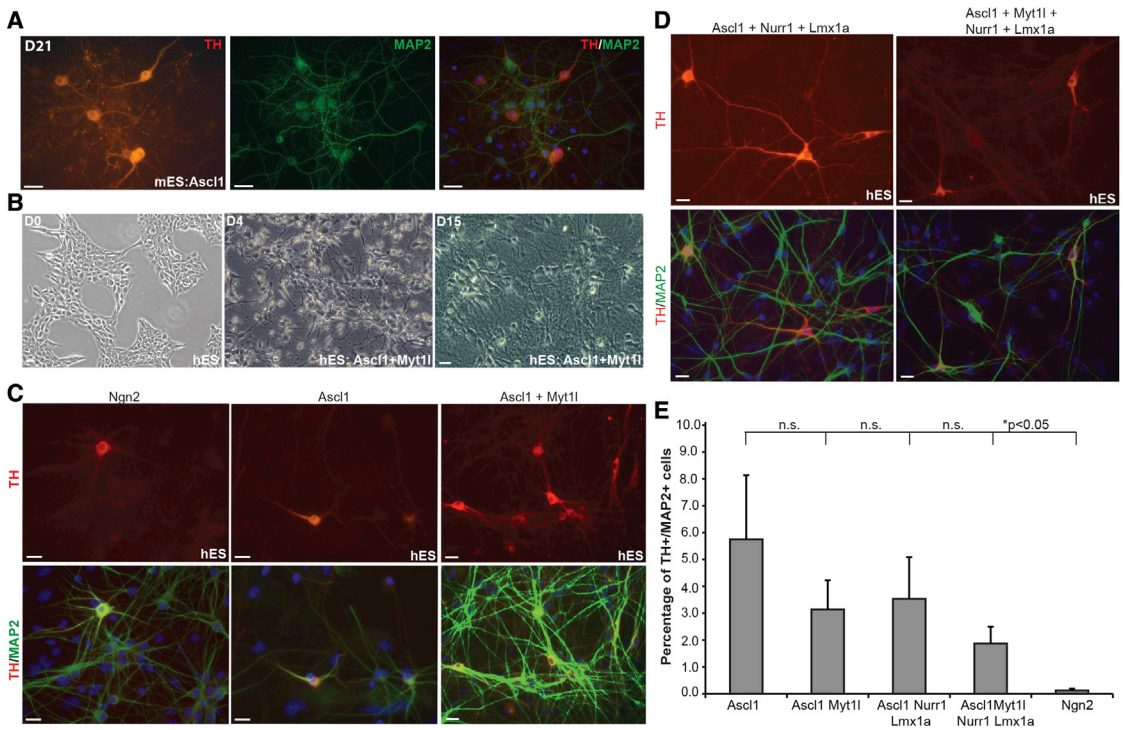

Figure 1. *Ascl1* is sufficient to induce TH$^+$ cells from ESCs

(A) Induction of TH$^+$MAP2$^+$ cells in mouse ESCs infected with *Ascl1* alone.

(B) Representative images illustrating the progression of human ES-iN cell induction at various time points as previously described (Zhang et al., 2013).

(C) H9 human ESCs infected with bHLH TF *Ngn2* cDNA alone produced rare TH$^+$ cells. H9 human ESCs infected with *Ascl1* robustly induced TH$^+$ cells. The addition of *Myt1l* improved the morphology of iN cells.

(D) Addition of dopaminergic TFs also induced TH$^+$ cells but did not increase the proportion of TH$^+$ cells among iN cells.

(E) Quantification of TH$^+$ iN cells among all MAP2$^+$ iN cells under the conditions indicated. Data are presented as mean ± SD (n = 3 independent experiments); Asterisk indicates significant difference (Student's t test,*p < 0.05); n.s., not significant.

Scale bars, 20 μm.

Accordingly, not a single TH$^+$ cell derived with *Ascl1* co-expressed the midbrain marker EN1.

As mouse and human ESCs are considered to represent different pluripotent states, the "naive" and "primed" state, respectively (Nichols and Smith, 2009), the expression of lineage-determining TFs could have differential effects. We therefore asked whether *Ascl1*-mediated induced TH$^+$ cells might have a different regional specification in mouse and human cells. However, similar to mouse ESCs, we found that about one-third of TH$^+$MAP2$^+$ human ES-iN cells were positive for PRPH, and no EN1$^+$ cells could be detected (Figures 2B and S2E).

We next asked whether the addition of critical midbrain dopamine neuron TFs—while not changing the overall numbers of TH$^+$ cells—would at least induce a central identity when co-expressed with *Ascl1* in human ESCs. We co-infected *Ascl1* with *Nurr1* and *Lmx1a*, and observed iN cells with a very similar peripheral marker profile as iN cells generated with *Ascl1* alone (Figure 2B). Moreover, we noted that the addition of *Myt1l* does not skew the ES-iN cells toward a CNS fate. In all conditions, about one-third of the TH$^+$ cells were PRPH$^+$ and none of the cells were EN1$^+$ (Figures 2B and S2E). Therefore, the addition of the midbrain-specific combination of *Nurr1* and *Lmx1a* was not sufficient to induce midbrain-type dopamine neurons from ESCs.

WNT1 signaling further improves the transcription factor-mediated formation of TH$^+$ cells

Given the limited effects of the candidate factors *Nurr1* and *Lmx1a*, we sought to screen a larger number of candidate factors to improve the generation of TH$^+$ cells from human ESCs systematically. We identified and cloned eight additional factors implied in dopamine neuron specification: *β-catenin*, *En1*, *FoxA2*, *Msx1*, *Otx2*, *Pitx3*, *Wnt1*, and *Wnt5*. We combined each of the ten candidate factors with *Ascl1* and *Myt1l* in three-factor pools and infected human

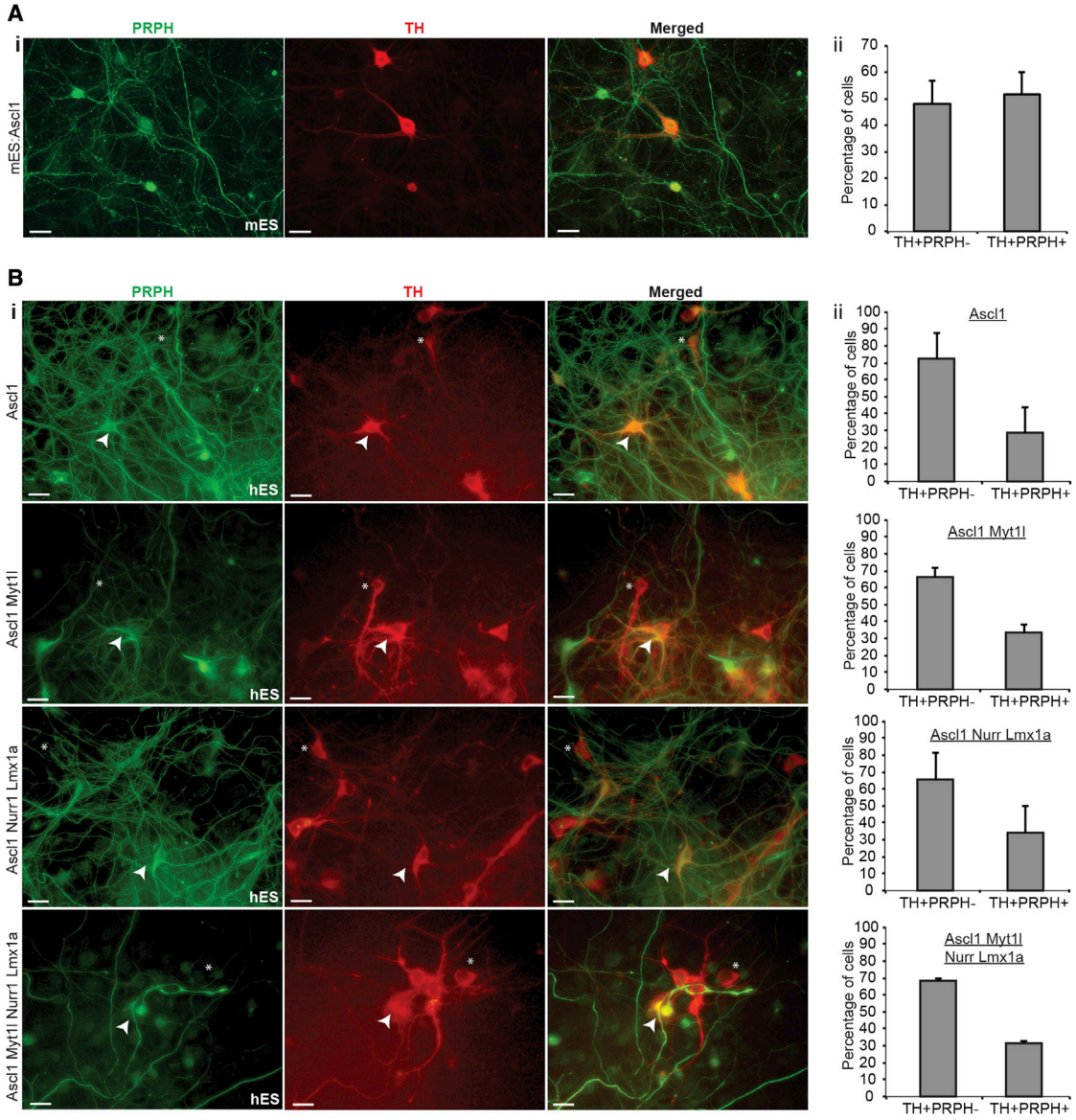

Figure 2. TH$^+$ ES-iN cells have features of peripheral neurons

(A) (i) The single factor *Ascl1* induced TH$^+$PRPH$^+$ double-positive cells in mouse ESCs. (ii) Quantification of TH$^+$ and PRPH$^-$ cells and TH$^+$PRPH$^+$ double-positive cells in mouse ESCs infected with *Ascl1* alone.

(B) (i) PRPH and TH co-expression (white arrowheads) was detectable even when the midbrain factors *Nurr1* and *Lmx1a* were added to the combination in human ESCs. TH$^+$ and PRPH$^-$ cells are indicated by white asterisks. (ii) Quantification of TH$^+$ and PRPH$^-$ cells, and TH$^+$PRPH$^+$ double-positive cells under all conditions.

Data are presented as mean ± SD (n = 3 independent experiments). Scale bars, 20 μm.

ESCs. As seen in previous combinations, neither *Nurr1* nor *Lmx1a* alone significantly increased the fraction of TH$^+$ cells (Figure 3A). Surprisingly, none of the additional candidate TFs increased the formation of TH$^+$ cells either. Instead, the expression of the *Wnt1* cDNA in ES-iN cells did so significantly (Figure 3A).

We sought to verify the WNT1 effects and test whether exogenously supplied WNT1 would be able to mimic the effects seen with the *Wnt1* virus. First, we treated the cultures with commercially available WNT3A protein and, similar to *Wnt5* virus, did not observe a beneficial effect, suggesting that the increased TH$^+$ iN cell formation is a specific effect of *Wnt1*. We therefore infected mouse embryonic fibroblasts (MEFs) with *Wnt1* lentivirus and co-cultured these MEFs in insets together with *Ascl1/Myt1l*-infected human ESCs in a way that only secreted factors

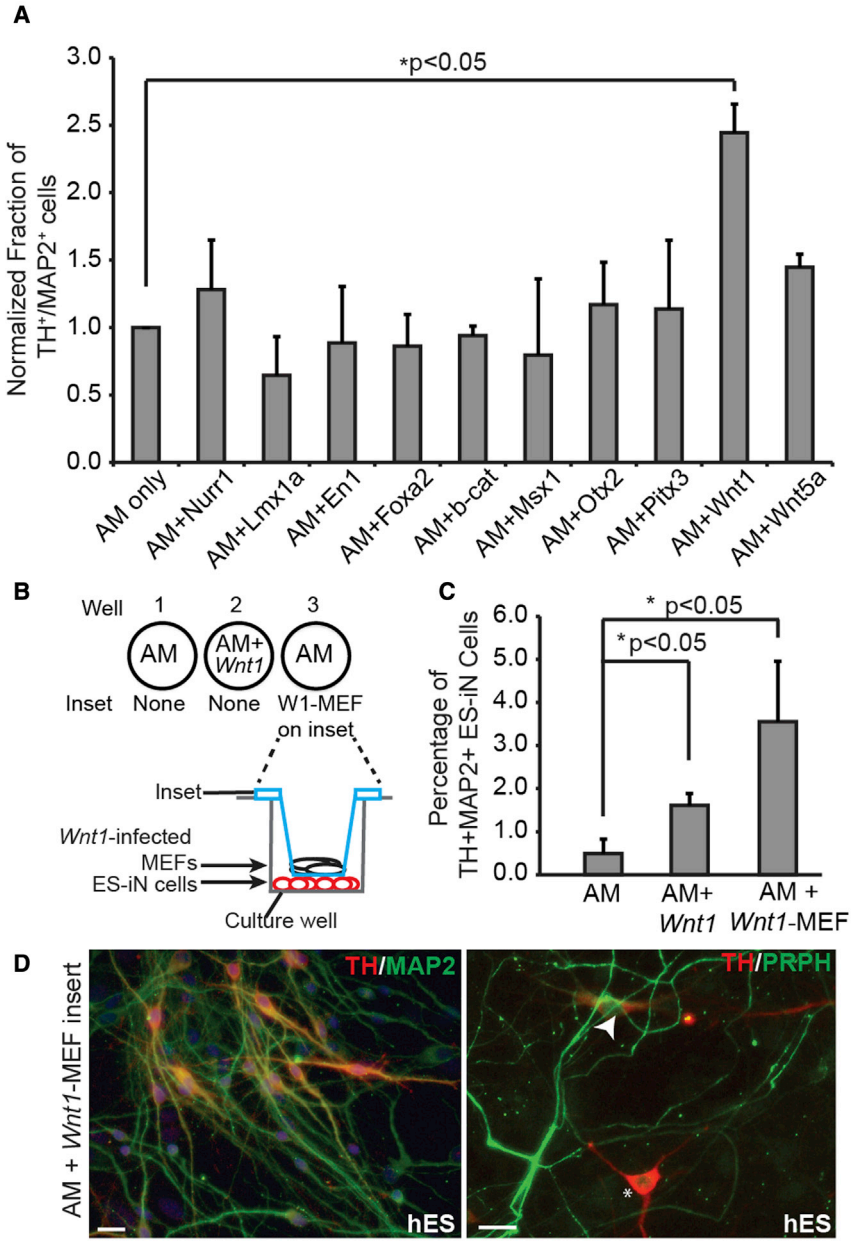

Figure 3. WNT1 improves the generation of TH$^+$ ES-iN cells

(A) Result of *Ascl* and *Myt1l* (AM) + 1 factor screen in human ESCs. Shown is the fraction of TH$^+$MAP2$^+$ cells among all MAP2$^+$ cells in various combinations normalized to the condition AM. Data are presented as mean ± SD (n = 3 independent experiments); Asterisk indicates significant difference (Student's t test, *p< 0.05).

(B) Diagram illustrating WNT1 delivery to the media via *Wnt1* cDNA-infected MEFs as a separate inset.

(C) Percentage of TH$^+$MAP2$^+$ cells in AM-only cells, AM + *Wnt1*-infected cells, and AM cells with *Wnt1*-infected MEFs inset. Data are presented as mean ± SD (n = 3 independent experiments). Asterisk indicates significant difference (Student's t test, *p< 0.05).

(D) TH$^+$MAP2$^+$ double-positive cells were induced in AM with *Wnt1*-MEF condition. Both TH$^+$PRPH$^+$ double-positive (white arrowhead) and TH$^+$ and PRPH$^-$ cells (white asterisk) were induced in AM with *Wnt1*-MEF condition. Scale bars, 20 μm.

could be exchanged between the MEFs and the forming iN cells (Figure 3B). Reassuringly, this way to deliver exogenous WNT1 yielded even more TH$^+$ cells than lentiviral delivery to ES-iN cells (Figure 3C), confirming that paracrine stimulation of the WNT1 pathway in developing iN cells supports the induction of TH$^+$ cells independent of viral infection.

Finally, we explored whether the WNT1 treatment would influence the central versus peripheral regional identity of TH$^+$ iN cells. Immunofluorescence analysis revealed that WNT1 treatment had no effect on regional specification. Similar to control conditions, many cells were PRPH$^+$ and none were EN1$^+$ (Figure 3D).

The neurotrophic factors BDNF and GDNF are crucial for transcription factor-mediated induction of TH$^+$ cells from ESCs

Our neuronal culture media typically contain neurotrophic factors to facilitate neuronal maturation and survival, but these growth factors are not predicted to influence cell-lineage specification. In one set of experiments we accidentally omitted them from the media when inducing human ESCs

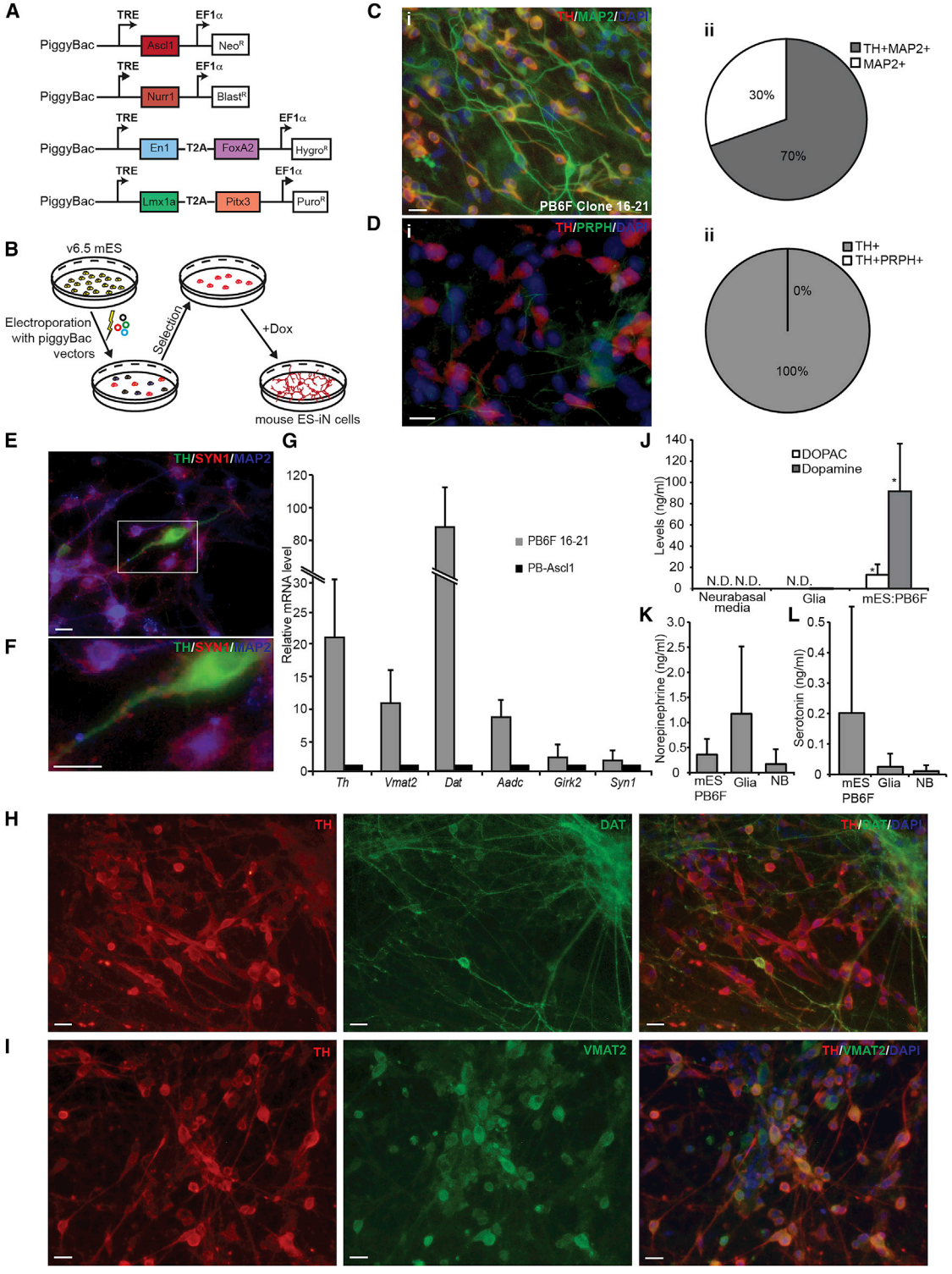

Figure 4. Induction of central dopamine iN cells from mouse ESCs

(A) Design of piggyBac vectors containing the different TFs and selectable resistance markers.

(B) Illustration of protocol to obtain multi-TF expressing ESCs and subsequent conversion to iN cells.

(C) (i) Expression of $TH^{+}MAP2^{+}$ iN cells, (ii) Quantification of $TH^{+}MAP2^{+}$ double-positive cells. Scale bar, 20 μm.

(legend continued on next page)

with *Ascl1* and *Myt1l* and failed to observe TH expression. We therefore repeated this experiment with the proper controls. While the overall number of MAP2$^+$ cells was not affected and iN cells had comparably mature neuronal morphologies, the fraction of TH$^+$ cells was dramatically decreased (Figure S3A). We conclude that brain-derived neurotrophic factor (BDNF)/glial cell line-derived neurotrophic factor (GDNF) signaling is essential to generate TH$^+$ iN cells from human ESCs, and the addition of these neurotrophic factors has a more profound effect than the lineage-specific TFs tested.

Co-expression of multiple midbrain-specific factors induces functional dopaminergic iN cells with a central neuronal identity from ESCs

Thus far, all modifications to our protocol to generate TH$^+$ cells from ESCs have yielded cells with peripheral and no CNS features. Several previous studies have identified various TF combinations to yield TH$^+$ cells of unknown regional identity from fibroblasts, but one of the studies observed the induction of the midbrain dopamine marker PITX3 using the combination of the six factors *Ascl1*, *Nurr1*, *Lmx1a*, *En1*, *FoxA2*, and *Pitx3* (Caiazzo et al., 2011; Kim et al., 2011; Pfisterer et al., 2011; Theka et al., 2013). We confirmed that *En1* and *Foxa2* together were sufficient to induce the expression of endogenous PITX3 in MEFs (Figures S3B and S3C). However, the number of PITX3$^+$TH$^+$ double-positive cells was extremely low, most likely because of the number of viruses used and difficulty in delivering so many TFs to the majority of cells.

We therefore asked whether a combination of all six midbrain-specific TFs, simultaneously expressed on the single-cell level, would be able to skew the lineage induction toward a CNS fate. To this end, we first needed to develop a system that would allow the non-trivial task of co-expressing six different transgenes in ESCs. Given the ease to grow mouse ESCs as single cells, we first attempted to generate mouse ESC clones with inducible expression of *Ascl1*, *Nurr1*, *Lmx1a*, *En1*, *FoxA2*, and *Pitx3*. To that end, we tested various possible ways to combine two cDNAs in one expression unit utilizing the self-cleaving 2A peptide system (Donnelly et al., 2001; Ryan et al., 1991). All bicistronic vectors generated were tested for cleavage efficiency based on immunoblotting after transfection or infection. We observed that linking *Ascl1* with *Nurr1* in either order resulted in ineffective cleavage and predominant expression of a fusion protein (ASCL1-T2A-NURR1) or low expression (NURR1-T2A-ASCL1) (Figure S3D). Thus, co-expression of those two cDNAs using the 2A peptide system was not feasible, and we kept them in separate expression units. In contrast, by arranging *En1* followed by *FoxA2* (EN1-T2A-FOXA2) and *Lmx1a* followed by *Pitx3* (LMX1A-T2A-PITX3), we were able to obtain efficient induction and cleavage (Figures S3E and S3F). We therefore reduced the number of required expression units to four, which became readily feasible with four different drug-resistance cassettes. We cloned the cDNAs into four doxycycline (dox)-inducible piggyBac expression vectors with four different selection cassettes: neomycin, blasticidin, hygromycin, and puromycin (Figure 4A). We co-transfected these plasmids together with a transposase plasmid and selected individual multiresistant clones (Figure 4B). After evaluating 24 clones for their neuronal induction efficiency (Figures S4A and S4B) and sustained homogeneous induction of all TFs (Figure S4C), we selected the clone with strongest induction potential for further characterization. Indeed, these cells had a high neuronal induction rate: 70% of the MAP2$^+$ iN cells were also TH$^+$ (Figure 4C) and very few were PRPH$^+$ (Figure 4D). Moreover, we could detect many SYN1$^+$ puncta along the dendrites (Figures 4E and 4F), and all TH$^+$ iN cells were still expressing the six TFs (Figures S4D–S4F). These results demonstrate that additional lineage-specifying TFs further optimize the regional specification of reprogrammed cells, and co-expression of a total of six factors in four expression units induces TH$^+$ neurons of central identity. Moreover, using quantitative RT-PCR (qRT-PCR), we observed that the dopamine markers *Th*, *Vmat2*, *Dat*, *Aadc*, and *Girk2* were expressed to higher levels than in *Ascl1*-induced ES-iN cells (Figure 4G). Immunofluorescence analysis showed that the TH$^+$ cells also expressed DAT and VMAT2 (Figures 4H and 4I). High-performance liquid chromatography (HPLC) analysis showed that these

(D) (i) Expression of PRPH$^+$ cells. Rare PRPH$^+$ cells were observed, but none were TH$^+$PRPH$^+$ double positive. (ii) Quantification of TH$^+$PRPH$^+$ cells. Scale bar, 20 μm.
(E) TH$^+$ PB6F mouse ES-iN cells were also immunoreactive for MAP2 and synapsin (SYN1). Scale bar, 20 μm.
(F) TH$^+$ PB6F mouse ES-iN cells also displayed punctate staining for SYN1. Scale bar, 20 μm.
(G) qRT-PCR analysis of mRNA levels of *Th*, *Vmat2*, *Dat*, *Aadc*, *Girk2*, and *Syn1*, normalized to *Ascl1* mouse ES-iN cells.
(H) TH$^+$ PB6F mouse ES-iN cells were immunoreactive for DAT. Scale bars, 20 μm.
(I) TH$^+$ PB6F mouse ES-iN cells were immunoreactive for VMAT2. Scale bars, 20 μm.
(J) HPLC analysis of dopamine and its metabolite DOPAC in PB6F mouse ES-iN cells.
(K) HPLC analysis of norepinephrine in PB6F mouse ES-iN cells.
(L) HPLC analysis of serotonin in PB6F mouse ES-iN cells.
Data are presented as mean ± SD (n = 3 independent experiments); Asterisk indicates significant difference (Student's t test, *p< 0.05).

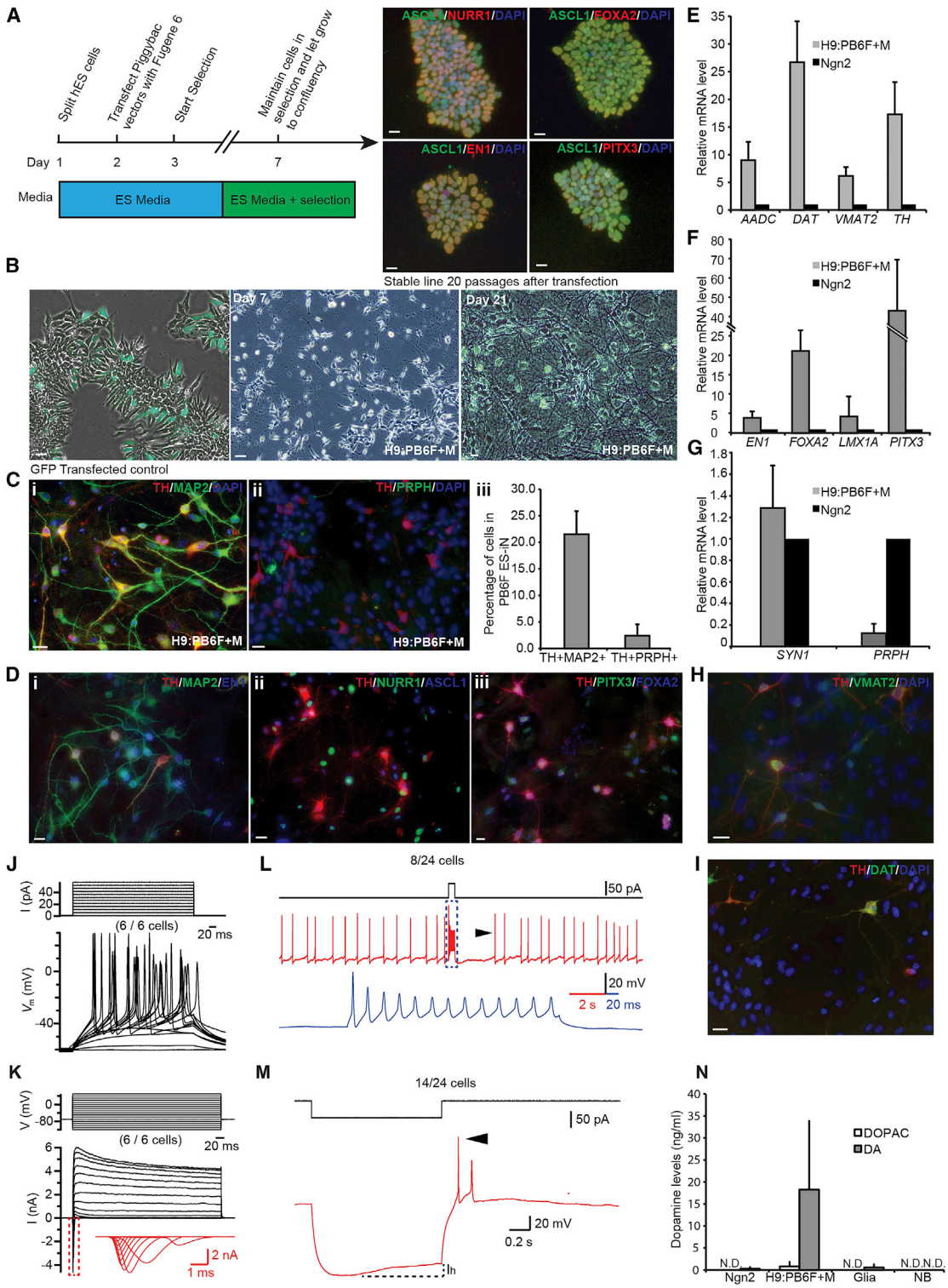

Figure 5. Induction of central, functional dopamine iN cells from human ESCs

(A) Timeline of establishing human ESC piggyBac lines. A polyclonal H9 piggyBac line (PB6F) showed homogeneous induction of all TFs after dox induction. Scale bars, 20 μm.

(B) Representative images illustrating the progressive morphological changes of PB6F human ES-iN cells following dox treatment similar to *Ngn2*-mediated conversion (Zhang et al., 2013). Scale bars, 20 μm.

(legend continued on next page)

six-factor mouse ES-iN cells produce dopamine and the dopamine metabolite, DOPAC (Figure 4J), with insignificant amounts of norepinephrine and serotonin (Figures 4K and 4L).

We also observed that the relative induction dynamics and levels of the TFs are extremely critical. Clones that were stably transfected with homogeneously inducible three piggyBac expression cassettes except *Nurr1* generated many TH^+ cells that were $MAP2^-$ and lacked neuronal morphologies when *Nurr1* was delivered using a lentivirus (Figures S4G and S4H).

Next, we sought to accomplish an equivalent induction of CNS dopamine neurons from human ESCs. These cells are difficult to grow as single cells, and we initially evaluated lentiviral gene delivery. However, the dox-inducible vectors that we modified to express constitutive selection marker to create inducible ESC lines for all six factors showed pronounced silencing of the inducible transgenes after multiple passages despite maintenance of drug resistance (Figures S5A–S5C). Therefore, we utilized the piggyBac induction system that was successfully used in mouse cells. After co-transfection, we generated a polyclonal population that induced the four expression cassettes homogeneously (Figures 5A and 5B). In contrast to the lentiviral delivery system, the piggyBac lines still showed expression of the TFs after multiple passages (Figure 5A). The piggyBac line, termed PB6F, was able to induce neuronal cells rapidly in the presence of *Myt1l* (Figure 5B). Similar to the mouse system, after induction of all six transgenes, a substantial fraction of $MAP2^+$ cells expressed TH and only a negligible fraction of the TH^+ iN cells expressed PRPH (Figure 5C). The expression of the reprogramming factors was maintained in the TH^+ iN cells (Figure 5D).

The high fraction of TH^+ cells in the population of iN cells allowed us to further characterize the cells on the bulk RNA level. We first confirmed that the pluripotency genes *OCT4* and *NANOG* were turned off in the PB6F ES-iN cells compared with undifferentiated ESCs (Figure S5D). We then analyzed the expression of characteristic dopamine neuron markers and observed the induction of *AADC*, a critical dopamine synthesis enzyme, and *DAT* and *VMAT2*, two dopamine transporters in the PB6F ES-iN cells when compared with *Ngn2* ES-iN cells (Figure 5E). Subsequently, we examined whether the endogenous genes for the midbrain-specific reprogramming factors were induced. Since they were expressed from viral transgenes, we designed primers specific to the 3′ UTRs of those genes and observed that *EN1*, *FOXA2*, *LMX1A*, and *PITX3* were well induced (Figure 5F). Notably, while the *SYN1* expression level was comparable with that in *Ngn2* ES-iN cells, the *PRPH* expression was much lower in the PB6F ES-iN cells, thus confirming our immunostaining results (Figure 5G). On the protein level, the PB6F ES-iN cells also expressed VMAT2 and DAT based on immunofluorescence analysis (Figures 5H and 5I).

Further electrophysiological characterization also showed that after more than 21 days after dox induction, when these cells were step-depolarized, action potentials could be detected (Figure 5J). These iN cells also expressed voltage-gated Na^+ and K^+ channels (Figure 5K). In addition,

(C) (i) Expression of TH and MAP2 in H9:PB6F+*Myt1l* ES-iN cells 3 weeks post induction (WPI). (ii) Only rare $PRPH^+$ cells were seen among TH^+ PB6F+*Myt1l* human ES-iN cells. (iii) Quantification of TH^+MAP2^+ double-positive and TH^+PRPH^+ double-positive cells in H9:PB6F+*Myt1l* human ES-iN cells. Data are presented as mean ± SD (n = 3 independent experiments). Scale bars, 20 μm.

(D) (i) Co-expression of TH, MAP2, and EN1. (ii) Co-expression of TH, NURR1, and ASCL1. (iii) Co-expression of TH, PITX3, and FOXA2. Scale bars, 20 μm.

(E) Relative mRNA levels of dopamine markers *AADC*, *DAT*, *VMAT2*, and *TH* in H9:PB6F+*Myt1l* ES-iN cells normalized to *Ngn2* ES-iN cells at 3 WPI.

(F) Relative mRNA levels of the endogenous *EN1*, *FOXA2*, *LMX1A*, and *PITX3* genes in H9:PB6F+*Myt1l* ES-iN cells normalized to *Ngn2* ES-iN cells.

(G) Relative expression of *SYN1* and *PRPH* in H9:PB6F+*Myt1l* ES-iN cells normalized to *Ngn2* ES-iN cells. Data are presented as mean ± SD (n = 3 independent experiments).

(H) Expression of VMAT2 in TH^+ H9:PB6F+*Myt1l* ES-iN cells at 3 WPI. Scale bar, 20 μm.

(I) Co-expression of DAT and TH in H9:PB6F+*Myt1l* ES-iN cells. Scale bar, 20 μm.

(J) Current-pulse (top) induced action-potential generation (bottom) in H9:PB6F human ES-iN cells at 3 WPI.

(K) H9:PB6F human ES-iN cells express voltage-gated Na^+ (inward current) and K^+ (outward current) channels. Inset: magnified view of the boxed area (red).

(L) Depolarizing current injection (upper black trace) into H9:PB6F+*Myt1l* ES-iN cells blocked the generation of action potentials, which then returned to baseline frequency after termination of current injection stimulus. The blue trace is expanded from the boxed area in the red trace.

(M) A hyperpolarizing current injection resulted in H9:PB6F+*Myt1l* ES-iN cell responding with hyperpolarization, a characteristic hyperpolarization sag mediated by h-current (Ih) and a short rebound delay.

(N) HPLC analysis of dopamine and its metabolite DOPAC in PB6F human ES-iN at 4 WPI, Ngn2 ES-iN cells, pure glial cultures, and Neurobasal medium (NB).

the cells exhibited other electrical properties typical of mesencephalic dopaminergic neurons, such as a depolarization block in response to positive current (Figure 5L) and a hyperpolarization sag in response to negative current injection indicative of pacemaker activity (Figure 5M).

Using HPLC analysis, we observed that the PB6F ES-iN cells produced dopamine and the dopamine metabolite DOPAC, both of which were either undetectable or extremely low in *Ngn2* ES-iN cells, glia-only cultures, or in the culture media (Figure 5N). Again, we found only small amounts of norepinephrine and serotonin in the PB6F ES-iN cell cultures (Figures S5E and S5F).

Next, we wanted to test whether all six factors were necessary to induce central dopamine neurons. To that end, we omitted each of the six factors separately and quantified the number of TH^+ and $PRPH^+$ cells. While there was no significant change in efficiency to generate TH^+ cells among the different conditions, there was an increase in TH^+PRPH^+ double-positive ES-iN cells in all five-factor conditions (Figures S5G and S5H). This result suggests that all six exogenous TFs cooperate to induce a CNS identity. Finally, to demonstrate the robustness of our approach and evaluate its application in iPSCs, we repeated the piggyBac induction system in three different human iPSC lines and observed comparable reprogramming efficiencies and low percentage of $PRPH^+$ cells (Figure S5I).

DISCUSSION

This report follows several previous publications that have shown that neuronal cells with many features of dopamine neurons, including expression of TH, the rate-limiting enzyme for catecholamine synthesis, can be directly generated from ESCs and fibroblasts using various combinations of TFs (Andersson et al., 2006; Caiazzo et al., 2011; Chung et al., 2009, 2012; Friling et al., 2009; Hong et al., 2014; Kim et al., 2011; Pfisterer et al., 2011; Theka et al., 2013). Our surprising observation that *Ascl1*, a proneural bHLH TF expressed in, but by no means restricted to, the midbrain, can induce TH^+ cells with similar (low) efficiencies as a previously reported combination containing two dopamine neuron-specific factors (Theka et al., 2013), raised the question of whether perhaps alternative TFs may improve the *Ascl1*-mediated TH induction. Surprisingly, we could not find any other single TF with that ability. In contrast, we identified specific extracellular signaling stimuli that had a dramatic effect on the efficiency of TH induction. In particular, WNT1, BDNF, and GDNF signaling promoted the *Ascl1*-induced generation of TH^+ cells. This result highlights the well-established notion that a specific status of the internal signaling pathway network can effectively modulate the cell biological effects of transcriptional regulators (Niehrs, 2012; Segal and Greenberg, 1996). Depending on the cellular environment in otherwise identical cells, the same TFs may have different effects on lineage specification.

Developmental studies have determined that *Ascl1* is expressed in newborn neurons of the central, the autonomic, and the enteric nervous system, and TH^+ cells are generated in all three compartments (Lo et al., 1997, 1998; Sommer et al., 1995). Therefore, another possible function of midbrain TFs or environmental signals, even if not modulating the overall efficiency of dopamine neuron generation, may be proper regional specification. We found that *Ascl1* primarily induces peripheral TH^+ cells from ESCs, suggesting an identity from either autonomic or enteric nervous system but excluding a central, midbrain identity. WNT1 is largely considered a dorsalizing stimulus except in the midbrain where dopamine neurons are born. It is therefore important for induction of both dorsal neural crest and (ventral) midbrain dopamine neurons (Arenas, 2014; Castelo-Branco et al., 2003; Danielian and McMahon, 1996; Garcia-Castro et al., 2002; Ikeya et al., 1997; McMahon and Bradley, 1990). Given this dual role, it is perhaps not surprising that while increasing the overall efficiency, WNT1 did not change the peripheral identity of *Ascl1*-induced cells significantly. What was surprising, however, was that *Lmx1a* and *Nurr1*, two well-characterized and highly specific midbrain TFs, in combination had no effect on central versus peripheral identity either.

This finding raised another, more fundamental question, namely whether the iN cell approach in general may lack the ability to properly install a region-specific trait in differentiating neurons. Improper regionalization would represent an important limitation of the iN cell technology, as only "authentic" midbrain dopamine neurons are considered to be able to integrate in a meaningful manner and restore dopamine function after transplantation (Lindvall and Bjorklund, 2011). This question prompted us to evaluate the effect of even more TFs. The combination of high integration rates of the piggyBac transposase system and availability of multiple drug selections allowed us to address this question by introducing a total of six well-characterized and proposed important TFs for midbrain dopamine neuron formation into both mouse and human ESCs. In both cases, the induction of the six factors resulted not only in a dramatic increase in the proportion of TH^+ neurons but, importantly, also in the absence of peripheral marker expression. This result is well compatible with the notion that the iN cell approach is able to induce proper regional fates, provided that the correct combination of TFs are identified. Another important insight from our work was that proper timing and levels of the TFs are critical for efficient and proper induction of neurons. This phenomenon may reflect the fact that the TFs used are also

sequentially expressed during normal development of the dopaminergic lineage (Ang, 2006; Burbach et al., 2003).

Another intriguing question that arises from our study is: what are the molecular determinants that lead to TH induction in a small population of equivalent cells with seemingly homogeneous *Ascl1* expression? The closely related bHLH TF *Ngn2* yielded only occasional TH^+ cells. Given the broad expression of *Ascl1* in the central and peripheral nervous system, it could be speculated that *Ascl1*, while being an important proneural TF, itself may lack subtype instructive potential and require other TFs and mechanisms to further specify neuronal subtypes.

Given their disease relevance, mesencephalic dopamine neurons are of high scientific interest. Our work demonstrates a new way to generate these cells with proper regional specification and in high purity from both mouse and human PSCs. TF programming of PSCs is more reproducible between different cell lines than conventional differentiation protocols, but delivery of TFs is more difficult than extracellular factors. Once a robust gene delivery system is worked out, such as the four-plasmid-piggyBac approach described in this work, it is straightforward to generate inducible cell lines. Expansion in the undifferentiated state followed by one-step conversion allows facile scaling of the production of a specific somatic cell type of interest in high purity and homogeneity. Our TF programming protocol will therefore be a valuable additional tool for the scientific community to generate central dopamine neurons from human PSCs.

EXPERIMENTAL PROCEDURES

Molecular cloning, cell culture, and viral infection

cDNAs for candidate genes were cloned into doxycycline-inducible lentiviral vectors. Human ESCs (H9) were cultured in either mTeSR1 (Stem Cell Technologies) or E8 (Invitrogen) and passaged when ~70% confluent. Murine ESCs were cultured in mouse ES medium (Dulbecco's modified Eagle's medium with 12% Knockout Serum Replacement (Invitrogen), 3% Cosmic Calf Serum (Thermo Scientific), and 1,000 U mL^{-1} leukemia inhibitory factor) on mitomycin C-treated (2 h treatment with 10 μg mL^{-1} mitomycin C, Sigma) MEF feeder cells and passaged when confluent. Replication-incompetent, vesicular stomatitis virus G-coated lentiviral particles were packaged in 293T cells as described by Wernig et al. (2008); 5×10^5 cells/well were plated in 6-well plates the day before. Both human and mouse ESCs were then infected in their respective culture medium containing polybrene (8 μg mL^{-1}, Sigma). After 16 h, the cells were switched to neural N3 medium containing doxycycline (2 μg mL^{-1}, Sigma) to induce gene expression as previously described (Wernig et al., 2002). Twenty-four hours after dox addition, medium was replaced with N3 containing dox and the appropriate antibiotic selection. After 72 h of selection, medium was switched to Neurobasal medium with B27 (Invitrogen) containing dox (antibiotic removal). After 48 h in Neurobasal medium, ES-iN cells were dissociated and replated on glial cultures and medium changed every 3–4 days with Neurobasal medium containing B27, dox (2 μg mL^{-1}), Ara-C (2 μM, Sigma), BDNF (20 ng mL^{-1}, R&D), and GDNF (20 ng mL^{-1}, R&D), unless otherwise noted.

piggyBac transfection of H9 ESCs and human iPSCs

Cells were dissociated and plated at a density of 5×10^5 cells/well of a 6-well plate the night before. The next day, cells were transfected using Fugene 6 (Promega) at a ratio of 3 μg DNA/9 μL Fugene 6. piggyBac vectors containing indicated transgenes were transfected together with a transposase plasmid (System Biosciences, CA). Twenty-four hours later, fresh medium containing antibiotic selection was added to cells. Cells were maintained in selection medium until establishment of stable lines.

Electroporation of piggyBac vectors into mouse ESCs

v6.5 mouse ESCs were maintained on mitomycin C-treated feeder cells. A 6-cm dish of almost confluent cells was dissociated with trypsin/EDTA and resuspended in Hank's buffered salt solution (Sigma). Twenty micrograms of piggyBac and 10 μg of transposase vector were mixed with the cell suspension in a 0.4-cm cuvette (Bio-Rad) and electroporated using a Bio-Rad Gene Pulser (0.55 kV, 25 μF). Cells were plated at different dilutions onto DR4 (Jackson Laboratories) mitomycin C-treated feeder cells. Cells were then maintained in selection medium until stably growing colonies were observed. Individual colonies were picked and tested for expression of various cDNA.

Immunofluorescence

Cells were fixed with 4% paraformaldehyde for 5 min and permeabilized with 0.2% Triton X-100/PBS. After blocking (4% BSA/1% Cosmic Calf Serum in PBS) for at least 30 min, primary antibodies were added and incubated overnight at 4°C. After three washes, secondary antibody conjugated with Alexa Fluor 488 or 555 (Molecular Probes) was added and incubated for 60 min. The wells were then incubated with 4′,6-diamidino-2-phenylindole (DAPI) nuclear counterstain for 5 min before analysis. Antibodies used were sheep anti-TH (Pel-Freez), mouse anti-EN1 (Development Studies Hybridoma Bank, IA), rabbit anti-PRPH (Millipore), mouse anti-MAP2 (Sigma), mouse anti-TUJ1 (Covance), rabbit anti-TUJ1 (Covance), rabbit anti-PITX3 (Invitrogen), rabbit anti-NURR1 (Santa Cruz Biotechnologies), goat anti-FOXA2 (Santa Cruz), mouse anti-SYN1 (Synaptic Systems), and rat anti-DAT (Millipore). See also Table S2.

Glial co-culture

Primary glial cultures were obtained from dissociated brains of 3-day-old pups and cultured for 2–3 passages before use (Pang et al., 2011; Vierbuchen et al., 2010). Glial cells were cultured in MEF medium or supplemented minimum essential medium containing B27 (Invitrogen), Apo-transferrin (Sigma), glucose (Sigma), insulin (Invitrogen), and fetal bovine serum (Atlanta Biologicals) as previously described (Maximov et al., 2007; Maximov and Sudhof, 2005), at a density of 1×10^5 cells/well of 24-well Matrigel-coated plates (Invitrogen). ES-iN cells were then plated at a density of 2×10^5 cells/well. All procedures involving animals were

performed according to protocols approved by Stanford University IACUC.

Co-culture with *Wnt1*-cDNA-infected MEFs

CD1 MEFs at passage 2 were plated at 1.5×10^6 cells in 10-cm tissue culture plates and infected with TetO-*Wnt1* lentivirus. The next day, dox was added and a GFP control plate verified successful infection. The *Wnt1*-cDNA-infected cells were then dissociated and plated at $5–6 \times 10^4$ cells/insert. After the MEFs had adhered to the membrane, the insert was transferred to the appropriate medium well.

Efficiency calculation

To reduce variation introduced by different virus batches, we normalized the number of TH^+ cells to the number of $MAP2^+$ cells per field. Twenty 20× fields were counted and the percentage of TH^+ cells among all $MAP2^+$ cells used as comparison between experiments. Cell quantification was measured either by eye or by ImageJ. Three independent experiments were carried out and Student's t test performed to examine statistical significance.

Quantitative RT-PCR

RNA was isolated using an RNeasy Kit (Qiagen) following the manufacturer's protocol and reverse transcribed using Superscript III (Invitrogen). Chosen primers were verified using appropriate positive and negative control samples (see Table S1).

Western blot

Cells were dissociated and lysed either in Laemmli buffer at 95°C or in lysis buffer (200 mM NaCl, 50 mM Tris pH 8.0, 1% Trion X-100, 5% glycerol). Protein lysate was run on a 4%–12% gradient Bis-Tris gel (Life Technologies) and electroblotted onto a polyvinylidene fluoride membrane. After blocking, the membrane was incubated with primary antibody for 1 h at room temperature, washed three times with PBS with 0.1% Tween 20, and incubated with secondary horseradish peroxidase antibody for 1 h at room temperature. Signal was detected using chemiluminescence on films (Western Lightning Plus enhanced chemiluminescence substrate, PerkinElmer).

HPLC

Cells were cultured in 24-well tissue culture dishes as described above. Cells were analyzed after 4 weeks or more in culture. Media and glia-only conditions were included as controls in the analysis for catecholamines and the metabolites. Cells were sent for HPLC analysis to the Neurochemistry Core at Vanderbilt University.

Electrophysiology

Electrophysiology experiments were performed as previously described (Chanda et al., 2013) on cultures 21 days post induction or later. In brief, current-clamp recordings were performed in whole-cell configuration with internal solution containing 130 mM $KMeSO_3$, 10 mM NaCl, 10 mM HEPES, 2 mM $MgCl_2$, 0.5 mM EGTA, 0.16 mM $CaCl_2$, 4 mM Na_2ATP, 0.4 mM NaGTP, and 14 mM Tris-creatine phosphate (pH adjusted with KOH to 7.3, 310 mOsm). The bath solution contained 140 mM NaCl, 5 mM KCl, 2 mM $CaCl_2$, 1 mM $MgCl_2$, 10 mM glucose, and 10 mM HEPES-NaOH (pH 7.4). Membrane potentials were maintained around −60 mV, and step currents were injected to elicit action potentials. Na^+/K^+ currents were recorded in voltage-clamp mode at a holding potential of −70 mV with step voltage changes as indicated (Figure 5).

SUPPLEMENTAL INFORMATION

Supplemental information can be found online at https://doi.org/10.1016/j.stemcr.2021.05.017.

AUTHOR CONTRIBUTIONS

Y.H.N. and M.W. conceived the project and designed the experiments; Y.H.N., S.C., J.A.J., N.Y., and Y.K. performed the experiments; Y.H.N. and S.C. analyzed the data; Y.H.N. and M.W. organized the figures; Y.H.N., T.C.S., and M.W. wrote the manuscript; all authors commented on the manuscript.

ACKNOWLEDGMENTS

Y.H.N. was supported by the Agency for Science, Technology and Research (A*STAR, Singapore). This study was funded by NIH grants R01 MH092931 and AG010770-18A1 (to M.W. and T.C.S.). T.C.S. is a Howard Hughes Medical Institute Investigator. M.W. was supported by the Tashia and John Morgridge Faculty Scholar Fund, Child Health Research Institute at Stanford, a New York Stem Cell Foundation-Robertson Investigator Award, and a Howard Hughes Medical Institute Faculty Scholarship.

Received: May 1, 2015
Revised: May 22, 2021
Accepted: May 23, 2021
Published: June 24, 2021

REFERENCES

Andersson, E., Tryggvason, U., Deng, Q., Friling, S., Alekseenko, Z., Robert, B., Perlmann, T., and Ericson, J. (2006). Identification of intrinsic determinants of midbrain dopamine neurons. Cell *124*, 393–405.

Ang, S.L. (2006). Transcriptional control of midbrain dopaminergic neuron development. Development *133*, 3499–3506.

Arenas, E. (2014). Wnt signaling in midbrain dopaminergic neuron development and regenerative medicine for Parkinson's disease. J. Mol. Cell Biol. *6*, 42–53.

Berninger, B., Costa, M.R., Koch, U., Schroeder, T., Sutor, B., Grothe, B., and Gotz, M. (2007). Functional properties of neurons derived from in vitro reprogrammed postnatal astroglia. J. Neurosci. *27*, 8654–8664.

Blanpain, C., Daley, G.Q., Hochedlinger, K., Passegue, E., Rossant, J., and Yamanaka, S. (2012). Stem cells assessed. Nat. Rev. Mol. Cell Biol. *13*, 471–476.

Burbach, J.P., Smits, S., and Smidt, M.P. (2003). Transcription factors in the development of midbrain dopamine neurons. Ann. N. Y Acad. Sci. *991*, 61–68.

Caiazzo, M., Dell'Anno, M.T., Dvoretskova, E., Lazarevic, D., Taverna, S., Leo, D., Sotnikova, T.D., Menegon, A., Roncaglia, P., Colciago, G., et al. (2011). Direct generation of functional dopaminergic neurons from mouse and human fibroblasts. Nature *476*, 224–227.

Castelo-Branco, G., Wagner, J., Rodriguez, F.J., Kele, J., Sousa, K., Rawal, N., Pasolli, H.A., Fuchs, E., Kitajewski, J., and Arenas, E. (2003). Differential regulation of midbrain dopaminergic neuron development by Wnt-1, Wnt-3a, and Wnt-5a. Proc. Natl. Acad. Sci. U S A *100*, 12747–12752.

Chambers, S.M., Fasano, C.A., Papapetrou, E.P., Tomishima, M., Sadelain, M., and Studer, L. (2009). Highly efficient neural conversion of human ES and iPS cells by dual inhibition of SMAD signaling. Nat. Biotechnol. *27*, 275–280.

Chanda, S., Ang, C.E., Davila, J., Pak, C., Mall, M., Lee, Q.Y., Ahlenius, H., Jung, S.W., Sudhof, T.C., and Wernig, M. (2014). Generation of induced neuronal cells by the single reprogramming factor ASCL1. Stem Cell Rep. *3*, 282–296.

Chanda, S., Marro, S., Wernig, M., and Sudhof, T.C. (2013). Neurons generated by direct conversion of fibroblasts reproduce synaptic phenotype caused by autism-associated neuroligin-3 mutation. Proc. Natl. Acad. Sci. U S A *110*, 16622–16627.

Chuhma, N., Zhang, H., Masson, J., Zhuang, X., Sulzer, D., Hen, R., and Rayport, S. (2004). Dopamine neurons mediate a fast excitatory signal via their glutamatergic synapses. J. Neurosci. *24*, 972–981.

Chung, S., Kim, C.H., and Kim, K.S. (2012). Lmx1a regulates dopamine transporter gene expression during ES cell differentiation and mouse embryonic development. J. Neurochem. *122*, 244–250.

Chung, S., Leung, A., Han, B.S., Chang, M.Y., Moon, J.I., Kim, C.H., Hong, S., Pruszak, J., Isacson, O., and Kim, K.S. (2009). Wnt1-lmx1a forms a novel autoregulatory loop and controls midbrain dopaminergic differentiation synergistically with the SHH-FoxA2 pathway. Cell Stem Cell *5*, 646–658.

Danielian, P.S., and McMahon, A.P. (1996). Engrailed-1 as a target of the Wnt-1 signalling pathway in vertebrate midbrain development. Nature *383*, 332–334.

Donnelly, M.L., Hughes, L.E., Luke, G., Mendoza, H., ten Dam, E., Gani, D., and Ryan, M.D. (2001). The 'cleavage' activities of foot-and-mouth disease virus 2A site-directed mutants and naturally occurring '2A-like' sequences. J. Gen. Virol. *82*, 1027–1041.

Eisenhofer, G., Kopin, I.J., and Goldstein, D.S. (2004). Catecholamine metabolism: a contemporary view with implications for physiology and medicine. Pharmacol. Rev. *56*, 331–349.

Friling, S., Andersson, E., Thompson, L.H., Jonsson, M.E., Hebsgaard, J.B., Nanou, E., Alekseenko, Z., Marklund, U., Kjellander, S., Volakakis, N., et al. (2009). Efficient production of mesencephalic dopamine neurons by Lmx1a expression in embryonic stem cells. Proc. Natl. Acad. Sci. U S A *106*, 7613–7618.

Garcia-Castro, M.I., Marcelle, C., and Bronner-Fraser, M. (2002). Ectodermal Wnt function as a neural crest inducer. Science *297*, 848–851.

Guillemot, F., Lo, L.C., Johnson, J.E., Auerbach, A., Anderson, D.J., and Joyner, A.L. (1993). Mammalian achaete-scute homolog 1 is required for the early development of olfactory and autonomic neurons. Cell *75*, 463–476.

Hanna, J.H., Saha, K., and Jaenisch, R. (2010). Pluripotency and cellular reprogramming: facts, hypotheses, unresolved issues. Cell *143*, 508–525.

Hong, S., Chung, S., Leung, K., Hwang, I., Moon, J., and Kim, K.S. (2014). Functional roles of Nurr1, Pitx3, and Lmx1a in neurogenesis and phenotype specification of dopamine neurons during in vitro differentiation of embryonic stem cells. Stem Cells Dev. *23*, 477–487.

Ikeya, M., Lee, S.M., Johnson, J.E., McMahon, A.P., and Takada, S. (1997). Wnt signalling required for expansion of neural crest and CNS progenitors. Nature *389*, 966–970.

Kim, J., Su, S.C., Wang, H., Cheng, A.W., Cassady, J.P., Lodato, M.A., Lengner, C.J., Chung, C.Y., Dawlaty, M.M., Tsai, L.H., et al. (2011). Functional integration of dopaminergic neurons directly converted from mouse fibroblasts. Cell Stem Cell *9*, 413–419.

Kriks, S., Shim, J.W., Piao, J., Ganat, Y.M., Wakeman, D.R., Xie, Z., Carrillo-Reid, L., Auyeung, G., Antonacci, C., Buch, A., et al. (2011). Dopamine neurons derived from human ES cells efficiently engraft in animal models of Parkinson's disease. Nature *480*, 547–551.

Lindvall, O., and Bjorklund, A. (2011). Cell therapeutics in Parkinson's disease. Neurotherapeutics *8*, 539–548.

Lo, L., Sommer, L., and Anderson, D.J. (1997). MASH1 maintains competence for BMP2-induced neuronal differentiation in post-migratory neural crest cells. Curr. Biol. *7*, 440–450.

Lo, L., Tiveron, M.C., and Anderson, D.J. (1998). MASH1 activates expression of the paired homeodomain transcription factor Phox2a, and couples pan-neuronal and subtype-specific components of autonomic neuronal identity. Development *125*, 609–620.

Maroof, A.M., Keros, S., Tyson, J.A., Ying, S.W., Ganat, Y.M., Merkle, F.T., Liu, B., Goulburn, A., Stanley, E.G., Elefanty, A.G., et al. (2013). Directed differentiation and functional maturation of cortical interneurons from human embryonic stem cells. Cell Stem Cell *12*, 559–572.

Marro, S., Pang, Z.P., Yang, N., Tsai, M.C., Qu, K., Chang, H.Y., Sudhof, T.C., and Wernig, M. (2011). Direct lineage conversion of terminally differentiated hepatocytes to functional neurons. Cell Stem Cell *9*, 374–382.

Maximov, A., Pang, Z.P., Tervo, D.G., and Sudhof, T.C. (2007). Monitoring synaptic transmission in primary neuronal cultures using local extracellular stimulation. J. Neurosci. Methods *161*, 75–87.

Maximov, A., and Sudhof, T.C. (2005). Autonomous function of synaptotagmin 1 in triggering synchronous release independent of asynchronous release. Neuron *48*, 547–554.

McMahon, A.P., and Bradley, A. (1990). The Wnt-1 (int-1) proto-oncogene is required for development of a large region of the mouse brain. Cell *62*, 1073–1085.

Merkle, F.T., Maroof, A., Wataya, T., Sasai, Y., Studer, L., Eggan, K., and Schier, A.F. (2015). Generation of neuropeptidergic hypothalamic neurons from human pluripotent stem cells. Development *142*, 633–643.

Nichols, J., and Smith, A. (2009). Naive and primed pluripotent states. Cell Stem Cell *4*, 487–492.

Niehrs, C. (2012). The complex world of WNT receptor signalling. Nat. Rev. Mol. Cell Biol. *13*, 767–779.

Okita, K., and Yamanaka, S. (2011). Induced pluripotent stem cells: opportunities and challenges. Philos. Trans. R. Soc. Lond. B Biol. Sci. *366*, 2198–2207.

Pang, Z.P., Yang, N., Vierbuchen, T., Ostermeier, A., Fuentes, D.R., Yang, T.Q., Citri, A., Sebastiano, V., Marro, S., Sudhof, T.C., et al. (2011). Induction of human neuronal cells by defined transcription factors. Nature *476*, 220–223.

Pfisterer, U., Wood, J., Nihlberg, K., Hallgren, O., Bjermer, L., Westergren-Thorsson, G., Lindvall, O., and Parmar, M. (2011). Efficient induction of functional neurons from adult human fibroblasts. Cell Cycle *10*, 3311–3316.

Qian, L., Huang, Y., Spencer, C.I., Foley, A., Vedantham, V., Liu, L., Conway, S.J., Fu, J.D., and Srivastava, D. (2012). In vivo reprogramming of murine cardiac fibroblasts into induced cardiomyocytes. Nature *485*, 593–598.

Ryan, M.D., King, A.M., and Thomas, G.P. (1991). Cleavage of foot-and-mouth disease virus polyprotein is mediated by residues located within a 19 amino acid sequence. J. Gen. Virol. *72*, 2727–2732.

Segal, R.A., and Greenberg, M.E. (1996). Intracellular signaling pathways activated by neurotrophic factors. Annu. Rev. Neurosci. *19*, 463–489.

Sommer, L., Shah, N., Rao, M., and Anderson, D.J. (1995). The cellular function of MASH1 in autonomic neurogenesis. Neuron *15*, 1245–1258.

Sulzer, D., Joyce, M.P., Lin, L., Geldwert, D., Haber, S.N., Hattori, T., and Rayport, S. (1998). Dopamine neurons make glutamatergic synapses in vitro. J. Neurosci. *18*, 4588–4602.

Theka, I., Caiazzo, M., Dvoretskova, E., Leo, D., Ungaro, F., Curreli, S., Manago, F., Dell'Anno, M.T., Pezzoli, G., Gainetdinov, R.R., et al. (2013). Rapid generation of functional dopaminergic neurons from human induced pluripotent stem cells through a single-step procedure using cell lineage transcription factors. Stem Cells Transl. Med *2*, 473–479.

Vierbuchen, T., Ostermeier, A., Pang, Z.P., Kokubu, Y., Sudhof, T.C., and Wernig, M. (2010). Direct conversion of fibroblasts to functional neurons by defined factors. Nature *463*, 1035–1041.

Wapinski, O.L., Vierbuchen, T., Qu, K., Lee, Q.Y., Chanda, S., Fuentes, D.R., Giresi, P.G., Ng, Y.H., Marro, S., Neff, N.F., et al. (2013). Hierarchical mechanisms for direct reprogramming of fibroblasts to neurons. Cell *155*, 621–635.

Wernig, M., Lengner, C.J., Hanna, J., Lodato, M.A., Steine, E., Foreman, R., Staerk, J., Markoulaki, S., and Jaenisch, R. (2008). A drug-inducible transgenic system for direct reprogramming of multiple somatic cell types. Nat. Biotechnol. *26*, 916–924.

Wernig, M., Tucker, K.L., Gornik, V., Schneiders, A., Buschwald, R., Wiestler, O.D., Barde, Y.A., and Brustle, O. (2002). Tau EGFP embryonic stem cells: an efficient tool for neuronal lineage selection and transplantation. J. Neurosci. Res. *69*, 918–924.

Xi, J., Liu, Y., Liu, H., Chen, H., Emborg, M.E., and Zhang, S.C. (2012). Specification of midbrain dopamine neurons from primate pluripotent stem cells. Stem Cells *30*, 1655–1663.

Yamamizu, K., Piao, Y., Sharov, A.A., Zsiros, V., Yu, H., Nakazawa, K., Schlessinger, D., and Ko, M.S. (2013). Identification of transcription factors for lineage-specific ESC differentiation. Stem Cell Rep. *1*, 545–559.

Yang, N., Chanda, S., Marro, S., Ng, Y.H., Janas, J.A., Haag, D., Ang, C.E., Tang, Y., Flores, Q., Mall, M., et al. (2017). Generation of pure GABAergic neurons by transcription factor programming. Nat. Methods *14*, 621–628.

Yoo, A.S., Sun, A.X., Li, L., Shcheglovitov, A., Portmann, T., Li, Y., Lee-Messer, C., Dolmetsch, R.E., Tsien, R.W., and Crabtree, G.R. (2011). MicroRNA-mediated conversion of human fibroblasts to neurons. Nature *476*, 228–231.

Zhang, Y., Pak, C., Han, Y., Ahlenius, H., Zhang, Z., Chanda, S., Marro, S., Patzke, C., Acuna, C., Covy, J., et al. (2013). Rapid single-step induction of functional neurons from human pluripotent stem cells. Neuron *78*, 785–798.